First-principles calculations of band-edge electronic states of silicon quantum wires

R. J. Needs and S. Bhattacharjee
Cavendish Laboratory, University of Cambridge, Cambridge CB3 0HE, United Kingdom

K. J. Nash
Defence Research Agency Malvern, Royal Signals and Radar Establishment, Malvern, Worcestershire WR14 3PS, United Kingdom

A. Qteish* and A. J. Read
Cavendish Laboratory, University of Cambridge, Cambridge CB3 0HE, United Kingdom

L. T. Canham
Defence Research Agency Malvern, Royal Signals and Radar Establishment, Malvern, Worcestershire WR14 3PS, United Kingdom
(Received 23 February 1994; revised manuscript received 6 June 1994)

Valence- and conduction-band-edge energies and effective masses of hydrogen-terminated silicon wires are calculated using a first-principles pseudopotential method, and the results are compared with effective-mass-theory (EMT) calculations. The first-principles result for the ordering of states at the valence-band maximum is different from the prediction of EMT. The magnitudes of the valence- and conduction-band effective masses for motion along the wire axis increase from their bulk values as the wire thickness decreases, but by much less than predicted by other calculations.

Recent experiments on porous Si, prepared by electrochemical etching of a Si wafer, have demonstrated efficient room-temperature visible photoluminescence.[1] The etching process produces material consisting mainly of columns or wires with widths ≤ 50 Å of crystalline Si with hydride-passivated surfaces.[2] The nature of the luminescence process is currently the subject of numerous experimental and theoretical studies. A number of different explanations have been offered, but detailed spectroscopy,[3] has recently demonstrated that the shorter photoluminescence (PL) wavelength of porous Si compared with bulk Si is due to quantum confinement of the electronic states within a crystalline Si structure.

First-principles pseudopotential calculations for hydrogen-passivated crystalline Si wires have shown that quantum confinement increases the minimum band-gap energy and leads to a direct gap at the center of the wire Brillouin zone.[4-4] Although even wide wires are nominally direct gap, the conduction-band-minimum wave functions retain a large projection onto states from near the Δ minimum of the bulk-Si conduction band. This is why one can observe phonon-assisted transitions, in which the bulk-Si crystal momentum is conserved.[3] The calculated band-gap energies are consistent with the PL energies obtained from experiments on comparable porous Si structures whose wire widths have been inferred from transmission-electron-microscopy (TEM) studies.[2] In addition, the zero-phonon radiative lifetime for recombination of localized excitons in a 16-Å-thick wire was calculated to be 560 μs,[8] which is in reasonable agreement with the value of ~ 130 μs estimated from experiments on comparable wires,[3] and is much longer than the radiative lifetime of 1 ns for bound excitons in the direct-gap semiconductor GaAs.[9]

Now that the quantum confined crystalline Si model is well established, it is important to study its predictions in more detail. In this paper, we report the results of first-principles calculations, which are used to develop the effective-mass theory (EMT) of Si wires, both by calculating effective masses and potential barrier heights for transport along a wire and by testing the validity of EMT based on bulk-Si properties alone. The technical details of our calculations are similar to those of our earlier work,[4] and the wire structures are identical to the ones studied there. We use a first-principles pseudopotential plane-wave technique and a supercell method in which a rectangular array of wires is used to restore three-dimensional periodicity. Each wire is rectangular in cross section with the wire axis along the [001] or z direction, and wire surfaces corresponding to (110)-type surfaces of bulk Si with each surface dangling bond passivated by a H atom. When viewed along the wire axis, the Si atoms form a rectangular array, and we study wires containing 72, 42, and 20 Si atoms per unit cell which form, respectively, 9×8, 7×6, and 5×4 arrays. The wires thickness is defined as $d=a_0(2M)^{1/2}/4$, where $a_0=5.429$ Å is the lattice constant of bulk Si and M is the number of Si atoms per unit cell, so that the wire thicknesses are $d\cong16.3$, 12.4, and 8.6 Å (the 8.6 Å or 5×4 wire is illustrated in Fig. 1 of Ref. 4). The shortest distance between H atoms on adjacent wires is 5 Å, so that the wires are well separated. The calculations for the Si wires were performed using a 6-Ry plane-wave cutoff, except for the 5×4 wire, for which the calculations were repeated with a 12-Ry cutoff as a test of the convergence. Calculations for bulk Si were performed with 6, 12, and 24-Ry cutoffs.

First, we study the nature of the states which form the valence-band maximum (VBM) of the wire structures.

0163-1829/94/50(19)/14223(5)/$06.00

We use EMT based on the Luttinger Hamiltonian without spin-orbit splitting for the sixfold degenerate (three orbitals and two spins) states of the VBM of bulk Si. We consider a square wire of side d with an [001] axis and (110)-type faces, using the particle-in-a-box model that the potential is constant inside the wire and infinite and repulsive outside. The VBM of bulk Si is formed from p-like orbitals, and the $k=0$ VBM states of the perfect wire structures defined above are either pure p_z states (where the z direction is along the wire axis), or pure p_x/p_y states (where the x and y directions are in the plane perpendicular to the wire axis). The effective masses associated with the confinement energy of the lowest p_z and twofold-degenerate p_x/p_y states are denoted by m_{cz} and m_{cxy}, and the EMT calculation gives, in terms of the Luttinger parameters γ_1 and γ_2:[10]

$$m_{cz}=(\gamma_1-2\gamma_2)^{-1}=0.277\ , \tag{1a}$$

$$m_{cxy}=0.219\ . \tag{1b}$$

The result for m_{cz} was obtained analytically by exact solution of the EMT equations, and was reported previously in Refs. 4 and 8, while the result for m_{cxy} was obtained by numerical solution of the EMT equations, which also predicts that a nondegenerate p_x/p_y state with a confinement mass of 0.237 occurs between the states described by Eq. (1). An approximate result for m_{cxy} of $(\gamma_1+\gamma_2)^{-1}=0.216$ can be obtained in simple EMT.[11] Because m_{cz} is larger than the confinement mass for all the other states within EMT the state at the VBM is of p_z character. The applicability of this result can be tested by analyzing the results of first-principles calculations. For the square $N\times N$ (N odd) wires studied by Ohno, Shiraishi, and Ogawa[6] and by Hybertsen and Needels,[7] the state at the VBM is twofold degenerate, and is of p_x/p_y character, in conflict with the EMT result.

We find a similar disagreement between EMT and first-principles calculations for our $N\times(N-1)$ (N odd) structures. The first-principles VBM state in these wires is a p_x/p_y state, but for wires with $N\geq 5$ the EMT VBM is a pure p_z state. The nature of the states close in energy to the VBM of the wire structures depends significantly on symmetry considerations.[7] The rectangular $N\times(N-1)$ (N odd) structures that we have studied have a single mirror plane parallel to the z axis of the wire and the short side of the rectangular cross section. Structures with different symmetries have been considered in other first-principles studies, including $N\times N$ (N odd) structures by Ohno, Shiraishi, and Ogawa[6] (note that these authors use a different convention for labeling their structures, so that[7] their $N\times N$ structure is equivalent to $(2N-1)\times(2N-1)$ in our notation) and by Hybertsen and Needels and the $N\times(N-1)$ structures with N even, also studied by Hybertsen and Needels. We have plotted the wave functions obtained from our first-principles calculations of the states close to the VBM and find that in each case the states are well described as being composed of p-like orbitals, with one state corresponding to the p_z state, and the other two being derived from the p orbitals aligned along the long and short sides of the rectangular cross section of the wire. For each of the wires that we have studied, the state derived from p orbitals pointing along the longer side of the rectangular cross section is the highest in energy, the p_z-like state is slightly lower in energy and the state derived from the p orbitals pointing along the shorter side of the rectangular cross section is lower again. We have also performed a limited set of calculations on an 11×10 wire structure, which also shows the same ordering of states at the VBM.

In conclusion, all of the first-principles results so far reported are mutually consistent with regard to ordering of the levels at the VBM, and all are in disagreement with EMT. Because the EMT overestimates the band-gap upshift by nearly 100% for the widest wire studied (20 Å),[4,8] the different ordering of the states at the valence-band maximum in EMT compared with the first-principles results is not particularly surprising. It is likely that the first-principles and EMT band orderings will be in agreement for thicker wires.

The EMT result for the conduction-band confinement mass m_{cc} for a square wire of side d with (110)-type faces is[4]

$$m_{cc}^{-1}=\tfrac{1}{2}\left[\frac{1}{m_T}+\frac{1}{m_L}\right]C\left[\frac{m_T}{m_L}\right]\ , \tag{2}$$

where a numerical calculation gives $C(m_T/m_L)=0.900$ for the experimental Si masses ($m_T=0.1905$ and $m_L=0.9163$), and $C(m_T/m_L)=1$ in simple EMT.[11] Equation (2) describes the conduction bands that are lowest in energy: these bands are derived from the $\pm[100]$, and $\pm[010]$ valleys in k space.[13,4] The total EMT band-gap upshift, calculated from the confinement masses of Eqs. (1a) and (2), was compared with the first-principles results in Ref. 5. From these results, we concluded that the EMT gives accurate values for the band-gap upshift for wire widths greater than about 33 Å.

In order to compare the results of our first-principles calculations with the separate predictions for the valence and conduction bands of Eqs. (1) and (2), we must locate a suitable reference energy level to measure the band energies with respect to. We have calculated the total electronic potential on the planes in the vacuum region precisely halfway between the wires, and averaged it over the planes to smooth out the small fluctuations and give the vacuum zero energy. The values of the band-edge energies measured with respect to this reference energy depend on the state of the surfaces of the wires which are hydrogen passivated. However, because the potential at the surfaces of the wires is essentially the same for all of our wires the changes in the band energies with wire thickness, measured with respect to the vacuum zero, derive from the quantum confinement and do not have a significant contribution from surface effects. The results for the valence- and conduction-band edges of the 9×8, 7×6, and 5×4 wires are plotted in Fig. 1. The EMT results of Eqs. (1a) and (2) are also plotted, which requires the location on the vertical axis of Fig. 1 of the position at which the band shifts go to zero. This was located by fitting two smooth curves to the first-principles results for

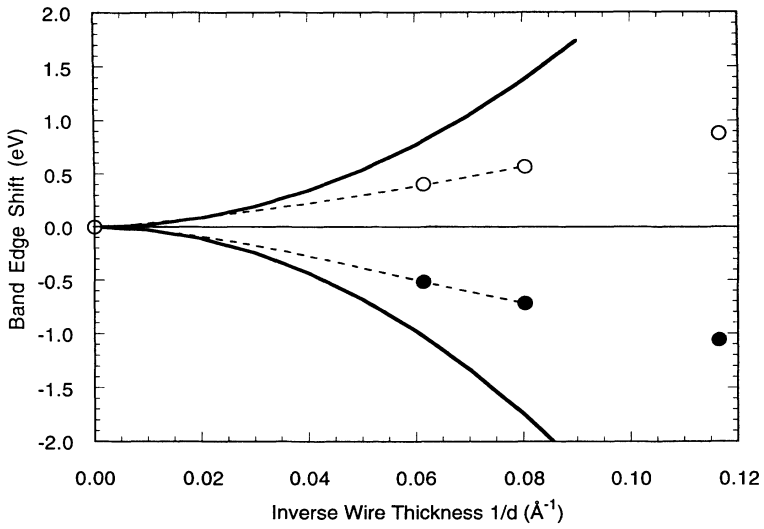

FIG. 1: The valence- (filled circles) and conduction-band-edge (open circles) shifts of the wire structures plotted against the inverse of the wire thickness. The effective-mass-theory shifts calculated from the masses of Eqs. (1a) and (2) are plotted as continuous curves. The dashed curves are interpolations passing through the first-principles results.

the valence and conduction bands, respectively, and extrapolating these curves to infinite wire thickness with the constraint that in this limit the curves must meet (i.e., the valence- and conduction-band shifts must both go to zero). The error in this extrapolation procedure is estimated to be less than 0.1 eV. Figure 1 shows that both the first-principles and EMT results predict that the band-gap upshift is divided roughly equally between the valence and conduction edges, in qualitative agreement with the photoemission and x-ray absorption measurements of Ref. 12, although the EMT overestimates the shifts for narrow wires.

We now turn our attention to the valence- and conduction-band effective masses for motion along the wire axis, which are not the same as the confinement masses of Eqs. (1) and (2). We denote the motional masses by m_{mz} and m_{mxy}, respectively, for the VBM p_z and p_x/p_y states of a square wire. In simple EMT[11] one finds

$$m_{mz} \cong (\gamma_1 + 4\gamma_2)^{-1} = 0.177 \ , \tag{3a}$$

$$m_{mxy} \cong (\gamma_1 - 2\gamma_2)^{-1} = 0.277 \ . \tag{3b}$$

The lowest conduction bands arise from $\pm[100]$ and $\pm[010]$ valleys and so have mass m_T for motion along the wire axis. These values apply in the limit of very wide wires, however, for wires of finite thickness these masses are altered by the folding over of the three-dimensional bulk band structure onto the axis along the wire direction. We have calculated the motional masses of bulk Si and of the wire structures using our first-principles technique. We calculated the band structure at a series of closely spaced points in k space along a line starting at the zone center and directed along the wire axis, and fitted the resulting energies to quadratic curves. Such calculations must be performed with care in order to avoid problems associated with the basis set changing from one k point to the next, which results in small jumps in the calculated band energies. To avoid this problem, we calculated the band energies of each wire structure at a number of points in reciprocal space within $0.005\ 2\pi/a_0$ of the zone center, but in fitting to the quadratic form we only took points that were calculated using exactly the same basis set. We also studied the effect on the masses of the anomalous band dispersion in the plane perpendicular to the wire axis, which is due to the small interactions between wires, by calculating the masses along the wire axis for various wave vectors within the plane perpendicular to the wire axis, however, the dependence was negligible. The anomalous dispersion of the states near the VBM is less than 10 meV in each case, which is much smaller than the energy splitting of the VBM states, which is greater than 61 meV in each case. The ordering of states at the VBM is, therefore, independent of the wave vector in the plane perpendicular to the wire axis. In Fig. 2, we plot the valence- and conduction-band motional effective masses of the wire structures and of bulk Si calculated along the wire axis [001] direction. The agreement between the calculated

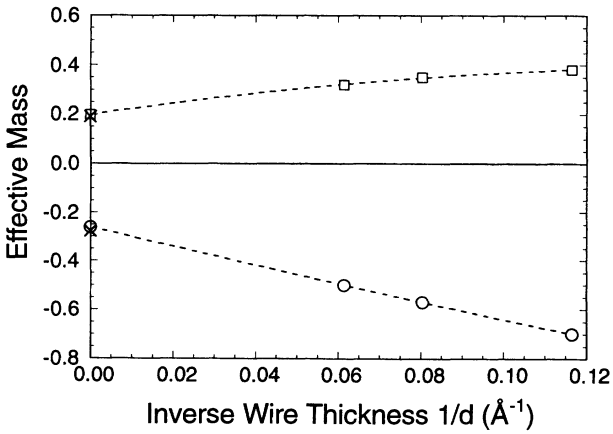

FIG. 2: Valence- (open circles) and conduction-band (open squares) effective masses of the wire structures and of bulk Si plotted against the inverse of the wire thickness. Experimental values for bulk Si (crosses) are also given; for the valence band the heavy-hole effective mass along the [001] direction [m_{mxy} of Eq. (3b)] is plotted, while for the conduction band, the transverse effective mass m_T is plotted.

and experimental values for bulk Si is good. The calculated conduction-band transverse effective mass for bulk Si of 0.199 is to be compared with the experimental value of $m_T=0.1905$, while the conduction-band longitudinal mass was calculated to be 1.01, in good agreement with the experimental value of $m_L=0.9163$. The p_x/p_y valence band is uppermost in the first-principles calculations, and so Eq. (3b) gives the appropriate mass in the (approximate) simple EMT model for comparison with the first-principles results. The mass given in Eq. (3b) is equal to the bulk-Si heavy-hole mass along [001], which we have calculated as 0.261, and which has an experimental value of 0.277. (Note that because the band structure of Si near the valence-band maximum is highly warped this is not equal to the density-of-states heavy-hole effective mass, which is $m_H=0.523$). From Fig. 2, we see that as the wires become thinner the magnitude of the valence- and conduction-band motional effective masses increase. The values obtained are, however, very different from the tight-binding results of Sanders and Chang,[13] who predicted that the magnitude of the valence-band effective mass for a wire width 23 Å (which is somewhat wider than our 16-Å-wide 9×8 wire) would be considerably greater than unity. Our calculated masses for the valence band are also significantly smaller than the first-principles results of Ohno, Shiraishi, and Ogawa.[6]

Our calculated effective masses and potential barrier heights for transport along the wire can be used in approximate EMT calculations. For example, the weak spin-orbit interaction can be treated in this way. For the highest VB state of the uniform 9×8 wire, this leads to a 4-meV energy shift, a 5% admixture of other zero-spin-orbit wave functions, and a correspondingly small correction to the effective mass. We discuss in more detail a more important application of EMT to the properties of Si wires, the description of the effects of fluctuations in the wire thickness along its length. TEM studies indicate that the wires undulate in thickness from 20 to 40 Å over a length scale of about 40 Å.[2] These fluctuations play an important role by enhancing the efficiency of the PL because they suppress nonradiative recombination of excitons by localizing the excitons, which might otherwise migrate to nonradiative centers.[4] If the motion along the wire is approximated by restricting it to the lowest subband, then the EMT equation separates into x, y, and z equations, and the z dependence (along the wire axis) of the conduction-band-minimum state is determined by

$$\left[-\frac{\hbar^2}{2}\frac{d}{dz}\frac{1}{m_{mc}(d)}\frac{d}{dz}+E_c(d)-E\right]\Psi_c(z)=0\ , \qquad (4)$$

where E is the energy measured with respect to the bulk conduction-band energy, $E_c(d)$ is the upshift of the conduction band due to the confinement within a wire of width d, which is itself a function of the position along the wire z, and m_{mc} is the conduction-band mass for motion along the z axis. (An analogous equation holds for the VBM with an appropriate change of mass and band energy). We model the shape of the undulating wire as a periodic array of overlapping spheres with diameter 40 Å and spacing $20\sqrt{3}$ Å, so that the wire thickness varies from 20 to 40 Å. For $1/d=0.025$ Å^{-1}, Figs. 1 and 2 give $E_c=0.12$ eV, $E_v=-0.14$ eV, $m_{mc}=0.25$ and $m_{mv}=-0.36$, while for $1/d=0.06$ Å^{-1}, we obtain $E_c=0.41$ eV, $E_v=-0.51$ eV, $m_{mc}=0.31$, and $m_{mv}=-0.49$. These values, which correspond to room-temperature band-gap energies of 1.36 and 2.02 eV, respectively, allow values of the parameters at intermediate wire thicknesses to be obtained by interpolation. Following Ref. 4 we apply our rectangular-wire values of $E_c(d)$ and $m_{mc}(d)$ by choosing d so that the cross-sectional are is the same as for the modeled wire, which has circular cross section. We find that the conduction-band maximum (VBM) state is 0.190 eV above (0.225 eV below) the bulk band edge. The lowest conduction band (highest valence band) has width 0.086 eV (0.044 eV) due to dispersion along the wire axis. Although these figures imply good conduction of electrons or holes along the wires, in practice transport will be impeded by strong localization effects, both in these bands and in the edges of the next conduction and valence bands, because the undulating wires have substantial irregularities, rather than the periodic structure assumed in our simple calculation.

In an undulating wire of arbitrary shape, hole mobilities will be lower than electron mobilities for two reasons. First, the hole mass is larger than the electron mass (Fig. 2). Second, the effective potential due to fluctuations in wire width is larger for holes than for electrons [Fig. 1 and Eq. (4)]. These factors explain, for example, why the bandwidth calculated for the periodic undulating wire is smaller for holes than for electrons.

In conclusion, we have calculated the valence- and conduction-band-edge energies and effective masses of three hydrogen-terminated silicon wires using a first-principles pseudopotential method, and compared with the results of effective-mass theory based on bulk-silicon parameters. The magnitudes of the valence- and conduction-band effective masses for motion along the wire axis increase from their bulk values as the wire thickness decreases, but by much less than predicted by other calculations. Our results provide essential information for a range of simple envelope-function calculations for Si wires, in particular for properties such as donor, acceptor, and exciton binding energies, electronic transport and localization.

S.B., A.J.R., and A.Q. thank DRA for financial support. The Cambridge group also thanks SERC for their continuing support.

*Present address: Centre for Theoretical and Applied Physics, Yarmouk University, Irbid, Jordan.

[1]L. T. Canham, Appl. Phys. Lett. **57**, 1046 (1990).

[2]A. G. Cullis and L. T. Canham, Nature **353**, 335 (1991).

[3]P. D. J. Calcott, K. J. Nash, L. T. Canham, M. J. Kane, and D. Brumhead, J. Phys. Condens. Matter **5**, L91 (1993); in *Microcrystalline Semiconductors: Materials Science and Devices,* edited by P. M. Fauchet, C. C. Tsai, L. T. Canham, I. Shimizu, and Y. Aoyagi, MRS Symposia Proceedings No. 283 (Materials Research Society, Pittsburgh, 1993), p. 143; J. Lumin. **57**, 257 (1993).

[4]A. J. Read, R. J. Needs, K. J. Nash, L. T. Canham, P. D. J. Calcott, and A. Qteish, Phys. Rev. Lett. **69**, 1232 (1992); **70**, 2050(E) (1993).

[5]F. Buda, J. Kohanoff, and M. Parrinello, Phys. Rev. Lett. **69**, 1272 (1992).

[6]T. Ohno, K. Shiraishi, and T. Ogawa, Phys. Rev. Lett. **69**, 2400 (1992).

[7]M. S. Hybertsen and M. Needels, Phys. Rev. B **48**, 4608 (1993).

[8]R. J. Needs, A. J. Read, K. J. Nash, S. Bhattacharjee, A. Qteish, L. T. Canham, and P. D. J. Calcott, Physica A **207**, 411 (1994).

[9]C. J. Hwang, Phys. Rev. B **8**, 646 (1973).

[10]*Physics of Group IV Elements and II-V Compounds,* edited by O. Madelung, Landolt-Börnstein, New Series, Group III, Vol. 17, Pt. a (Springer, New York, 1982), and references therein.

[11]By simple EMT we mean a variational calculation within EMT with a single envelope function, equal to the ground-state envelope function for the square wire with a single isotropic parabolic band. The basis functions for the variational calculation are given by this envelope function multiplied by each of the possible Bloch functions (for the valence band, these have p_x, p_y, and p_z character).

[12]T. van Buuren, T. Tiedje, J. R. Dahn, and B. M. Way, Appl. Phys. Lett. **63**, 2911 (1993).

[13]G. D. Sanders and Y.-C. Chang, Appl. Phys. Lett. **60**, 2525 (1992); Phys. Rev. B **45**, 9202 (1992).